Influence of longitudinal reinforcement and stiffeners on strength and behaviour of 3D wall panels under axial compression

P. Poluraju
PhD Scholar, Structural Engineering Division
Department of Civil Engineering
Indian Institute of Technology Madras, Chennai-600036, India.
rajupolup@gmail.com

G. Appa Rao
Professor, Structural Engineering Division,
Department of Civil Engineering,
Indian Institute of Technology Madras, Chennai-600036, India.
garao@iitm.ac.in

Abstract—**3D precast concrete sandwich panels are often used in building construction due to their better performance, thermal efficiency, and speed of construction. This paper reports on experimental studies on 3D panels made up of wythes of concrete on interior and exterior faces separated by 50 mm of lightweight insulation material to obtain typically 150 mm thickness. Performance of 3D panels under axial compression emphasizing the influence of parameters such as longitudinal reinforcement and stiffening elements has been investigated. Full-size and one-third size elements as slender and squat walls were tested. Load-deformation response, strain in steel connectors, crack formation and crack propagation under axial compressive loading were analyzed. Along with a brief review of literature, laboratory test results are compared with the existing code provisions such as current ACI design formula reported for solid walls to verify the validity of this empirical formula for sandwich 3D panels. The test results showed that the 3D panels exhibited composite behaviour under axial compression up to failure. The ultimate strength of 3D panels was found to decrease non-linearly with the increase in the slenderness ratio. Further, the addition of longitudinal reinforcement and stiffening elements showed better strength and deformability.**

Keywords: 3D panel; longitudinal reinforcement; stiffening elements; axial compression

I. INTRODUCTION

Construction systems based on sandwich panels are commonly used worldwide for intensive building production. Sandwich panels are typically two concrete layers which are separated by an internal insulation layer of various materials (i.e. expanded polystyrene) and are usually joined with "steel connectors" (i.e. truss connectors) able to transfer the longitudinal interface shear between the layers so as to ensure a fully-composite or a semi-composite behaviour of the sandwich panel [13]. 3D panel is a prefabricated panel, which consists of a super-insulated core of rigid expanded polystyrene sandwiched between two-engineered sheets of 2.5 mm diameter (Ø) with a tensile strength of 880 N/mm² steel welded wire fabric mesh. To achieve 3D panel, another 2.5 mm diameter galvanized steel truss wire is pierced through the polystyrene core at offset angles for superior strength and integrity, and welded to each of the outer layer sheets of eleven-gauge steel welded wire fabric mesh. The 3D panels

are used for numerous building applications including floor systems, ceilings and a roof structure. The 3D panel is an excellent product for building privacy walls around the home or building structure *(EVG)*. Schematic view of 3D panel is shown in Figure 1.
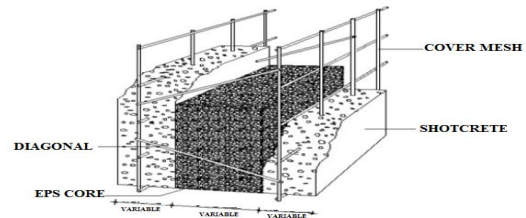

Figure 1. 3D Wire Panel Cross Section (EVG)

3D panels function as efficiently as precast solid walls but differ in their build-up. Interest in sandwich panels as load-bearing wall panels has been growing over the past few years because the manufacturers are looking for more viable products and architects/engineers are pleased with the structural and energy performance of the sandwich panels [14]. 3D sandwich wall panels acting as load bearing elements are structurally efficient, providing economical means of transferring floor and roof loads to the foundations. The structural behaviour of the panels depends greatly on the strength and stiffness of the connectors, while the thermal resistance of the insulation layer governs the insulation of the panel [4, 6, 12].

The complex behaviour of 3D sandwich panels due to its material non-linearity and the interaction between its various components has led researchers to rely on experimental investigations backed by simple analytical studies [6, 8, 12]. This may explain the lack of information on the behaviour of this important type of structure.

Experimental studies on 3D sandwich panels included pure shear tests and flexural tests as well as tests under combined shear and flexure [4, 8-12]. However, influence of longitudinal reinforcement and stiffeners of 3D sandwich panels under axial load have not been studied, thus emerges the need of current investigation. A review of studies on reinforced concrete solid wall panels as described below is,

therefore important, as the behaviour of 3D sandwich panels is often extrapolated from the behaviour of the reinforced concrete (RC) solid panels.

II. ACI EMPIRICAL WALL DESIGN METHOD

ACI 318-89 wall design equation
ACI 318-89 [2] gives the equation for the design axial load strength of a wall as

$$P_u = 0.55\phi\, f_{cu}\, A_c\, [1 - (kH/32t)^2] \qquad (1)$$

Eq. (1) specified by *ACI 318-89* [2] is applicable for walls restrained at the top and bottom with $H/t \leq 25$ or $L/t \leq 25$, whichever is less for load-bearing walls

Where A_c is the gross area of wall panel section (assumed equal to the gross concrete area); f_{cu} is characteristic cube strength of concrete; *H is* the effective height; $k = 0.8$ for walls restrained against rotation; $= 1.0$ for walls unrestrained against rotation; *L* is the width of the panel; *t is* the thickness of the panel section; and $\phi = 0.7$ for compression members.

It is evident from the review of literature that only some experimental investigations supported by simple analytical studies were carried out on the performance of 3D sandwich under flexure and shear [7]. There is however a better understanding of the behaviour of solid reinforced concrete panels. No studies were reported on the behavior with longitudinal reinforcement and stiffened sandwich wall panels under axial load.

In view of the limited published information on 3D sandwich wall panels as load bearing walls and its increasing usage in the construction industry, experimental and analytical investigations on 3D panels under axial load were calculated based on ACI design practice for solid wall panels.

III. EXPERIMENTAL CAMPAIGN

In this study experimental investigation has been divided in to two phases

A. Plain 3D Sandwich Wall Panels

3D sandwich plain wall panels of two different aspect ratios were investigated. Four panels were cast: two panels with 12 mm diameter (Φ) longitudinal reinforcement bars @ 300 mm c/c and two without longitudinal reinforcement were cast with M20 grade concrete. The geometric details of four panels and their designations are presented in Table I.

A square welded zinc coated galvanized steel mesh of 2.5 mm diameter wires with 50×50 mm (currently in use) openings was used as the longitudinal and transverse reinforcement for the inner and the outer wythes, while steel connectors running through the full height of the panels were used to tie the inner and the outer concrete wythes to improve the composite action (Fig. 2). These connectors were made of 2.5 mm diameter zinc coated galvanized steel wires bent to an angle of 45^0 [7]. Lightweight expanded polystyrene were used as the insulation material in the core as it is economical and readily available. The polystyrene sheet was cut into pieces and inserted between the inner and the outer wythes and between steel connectors. The material properties of the concrete and the steel used for steel connectors and reinforcement were tested in the laboratory and their properties are presented in Tables II and III respectively. For casting the specimen, the formwork was cleaned and placed on a plane floor. The concrete was then poured from manual mix to form the bottom wythe and compacted by vibration and above the concrete layer 3d skeleton was placed. 35 mm cover was maintained in both bottom and top wythe. The top wythe was then laid and fully compacted, its surface was trowelled to obtain a smooth finish. Three standard concrete cubes were prepared at the time of casting of 3D panels to determine the compressive strength of concrete. The stages of casting of 3D wall panel are shown in Fig. 3.

TABLE I. TEST SPECIMENS WITH DIMENSION, ASPECT RATIO AND SLENDERNESS RATIO

S.No	Panel	H (mm)	B (mm)	t (mm)	H/B	H/t	t_1 (mm)	t_2 (mm)	c (mm)	Remarks	Grade of Concrete
1	WP1-NR-AC	1250	1250	150	1	8.33	50	50	35	---	M20
2	WP1-WR-AC	1250	1250	150	1	8.33	50	50	35	5-12mm ø @ 300 c/c (Each side)	M20
3	WP2-NR-AC	3750	1250	150	3	25	50	50	35	---	M20
4	WP2-WR-AC	3750	1250	150	3	25	50	50	35	5-12mm ø @ 300 c/c (Each side)	M20

H, the panel height; *B,* the width; *t,* the overall thickness; t_1, thickness of each concrete wythe; t_2, the insulation thickness; *c,* the concrete cover; WP1, plain wall panel (squat wall); WP2, plain wall panel (slender wall); NR, no longitudinal reinforcement; WR, with longitudinal reinforcement; AC, axial compression load
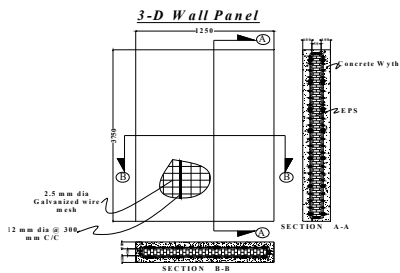

Figure 2. Typical 3D plain sandwich wall panel

Figure 3. Casting of 3D sandwich wall panel

TABLE II. CONCRETE PROPERTIES

Concrete		
f_{cu} (MPa)	f_t (MPa)	E_c (kN/mm^2)
36.42	4.22	30.17

f_{cu}, compressive concrete strength; f_t, tensile stress of concrete at failure; E_c, concrete modulus of elasticity.

TABLE III. PROPERTIES OF STEEL

Steel	Yield stress, f_y (MPa)	Stress at failure (MPa)	Strain at failure	E_s (kN/mm^2)
Wire mesh	658	710	0.05	142
Longitudinal rebar	490	556	0.031	158

f_y, yield stress of steel; E_s, steel modulus of elasticity
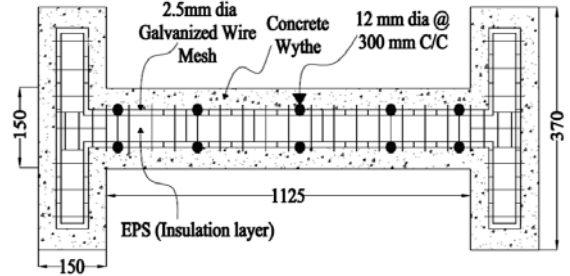
Figure 4. Plan, and cross sectional view of 3D sandwich stiffened panel.

TABLE IV. TEST SPECIMENS WITH DIMENSION, ASPECT RATIO AND SLENDERNESS RATIO

S. No	Panel	H (mm)	B (mm)	t (mm)	H/B	H/t	t_1 (mm)	t_2 (mm)	c (mm)	Remarks	Grade of Concrete
1	SWP1-NR-AC	1250	1425	150	0.87	8.33	50	50	35	---	M20
2	SWP1-WR-AC	1250	1425	150	0.87	8.33	50	50	35	5-12mm ø @ 300 c/c Stiffener- 370 × 150 mm	M20
3	SWP2-NR-AC	3750	1425	150	2.63	25	50	50	35	---	M20
4	SWP2-WR-AC	3750	1425	150	2.63	25	50	50	35	Same as above	M20

H, the panel height; B, the width; t, the overall thickness; t_1, thickness of each concrete wythe; t_2, the insulation thickness; c, the concrete cover; SWP1, stiffened wall panel (squat wall); SWP2, stiffened wall panel (slender wall); NR, no longitudinal reinforcement; WR, with longitudinal reinforcement; AC, axial compression load.

B. Stiffened 3D Sandwich Wall Panels

From the Literature review, it's clear that the 3D plain panels are lacking strength due to the buckling effect. To improve the stiffness of that panel, stiffeners are added to both ends of the 3D plain model as depicted in Fig. 4. Out of four panels two were provided with 12 mm diameter (Φ) longitudinal reinforcement bars @ 300 mm c/c and remaining two without longitudinal reinforcement bars were cast using M20 grade concrete. The details of panels with their designations, aspect ratio H/B and slenderness ratios H/t are shown in Table IV.

C. Instrumentation and Measurements

The response of the panel to the applied loading was observed through deformations, surface strains and strains in the embedded steel reinforcement.

Each panel (both plain and stiffened with and without longitudinal reinforcement, either squat or slender) is arranged with two LVDTs (S_{vf} and S_{vb}), with a range of ± 50 mm for squat walls and ± 100 mm for slender walls, applied in an extensometric configuration to measure the strain over a base length 0.416 m for squat walls and 1.25 m for slender walls. Three more transducers (S_1, S_2, S_3) are placed horizontally at ¼, ½ and ¾ height of the panel to measure the horizontal displacement of both squat and slender walls. Two transducers (S_4, S_5) were placed within the web thickness, at an angle 45^0 with respect to the vertical direction, at ¼ height for only plain wall panels, in order to measure the relative displacement between the concrete layers shown in Fig.5.
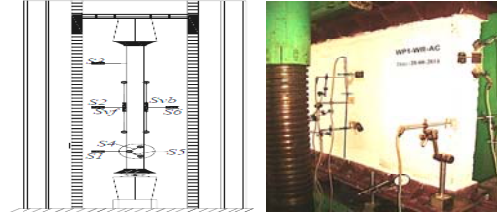

Figure 5. LVDTs position for wall panel

Both electrical strain gauges and Demountable Mechanical (DEMEC) gauge were used to measure the surface strains of embedded steel bars, wire mesh and concrete. The positions of electrical resistance strain gauges, metal pellets (to measure the strains using DEMEC gauge) are shown in Fig. 6. The pellets were fixed at the appropriate positions on the surface of panels, using resin type adhesive, after cleaning the surface with sand paper and acetone. Electrical resistance strain gauges of 5 mm gauge length with a resistance of 120 ± 0.3 ohms and a gauge factor 2.13 ± 1% were adopted. The electrical resistance strain gauges were fixed on reinforcement steel bars and wire mesh at the top, middle and bottom before casting of concrete. The gauges were fixed at the appropriate locations on the surface of the reinforcement steel bars, using resin adhesive after removing rebar ribs. Subsequently, the strain gauge location was made waterproofed. Crack widths were measured using a microscope having a least count of 0.05 mm. The axial load was recorded from the loading machine at constant load increments, which were fixed before the loads were applied.

(a)   (b)

Figure 6. (a) DEMEC pellets (b) Electric strain gauge

D. Test setup

Fig. 7 shows the loading frame used for testing the panels. The load was applied by 6000 kN Mohr and Federhaff compression testing machine. This machine has three loading ranges of 1200, 3000 and 6000 kN. All the panels were tested in vertical position. A leveling ruler (laser) was used to ensure proper leveling of the panel. The panels were tested with the bottom end pinned (cylindrical pin) and top end fixed. Load was applied through bottom platen of the machine (pinned end side). This is assumed to simulate the end conditions of the panel when used in a single storey building. The panel end supports were specially fabricated for axial load testing. A schematic sketch of the fabricated end support is shown in Fig. 8(a). It is made with steel plates and round rods to provide hinged condition at the supports. Each device was made with two parts labeled part-1 and part-2. Part-1 was made with two 200 mm × 1500 mm size 40 mm thick steel plates and 60 mm diameter one round steel rod, as shown in Fig. 8(b). A 200 mm width, 1500 mm length and 40 mm thick plate was taken and a segmental groove of depth 20 mm was made at the middle of the plate throughout its length in a lathe machine. On either side of this groove the corners of the plate were cut tapered to achieve 25 mm thickness at the edges and 40 mm thickness (i.e. full thickness) up to 20 mm away from the groove. Similarly, another plate was also made. On one plate either side of groove, 12 mm size screwed holes were made at the ends and at the middle, along the length of the plate to accommodate the bolts. A 60 mm diameter and 1500 mm long steel rod was accommodated in the groove, and above the rod, another plate was placed as shown in Fig. 8(b). Part-2 was made with 16 mm thick steel plates. The schematic diagram of this part is shown in Fig. 8(c). Plates of 16 mm thick, 400 mm width and 1300mm length 1300 mm were used for testing of plain wall panel, whereas for testing of stiffened wall panel, shown in Fig. 8(d), plates of 16 mm thick, 400 mm width and 1700mm length were used. Two 12 mm thick steel plates of width 100 mm and 1300mm length were welded symmetrically at the middle at a 150 mm clear spacing between them to form a channel. At the two ends, steel plates of 140 mm × 110 mm and 12 mm thick were welded. On either side of the channel, 12 mm thick trapezoidal shape stiffeners were welded. The assembled device (parts-1 and 2), corresponding to the bottom end support is shown in Fig. 8(d).
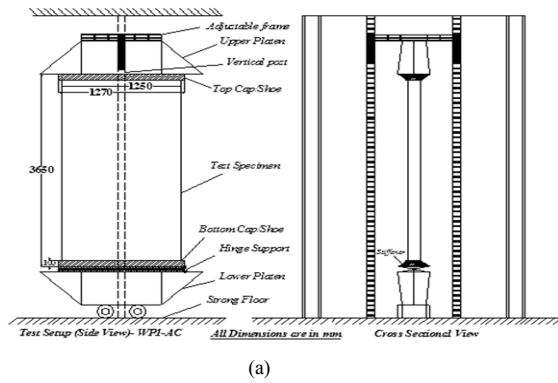

(a)

(b)

Figure 7. Plain wall panel (a) Schematic diagram (b) Test setup
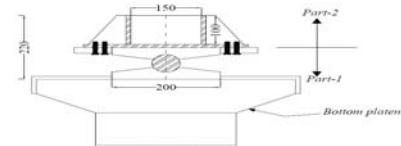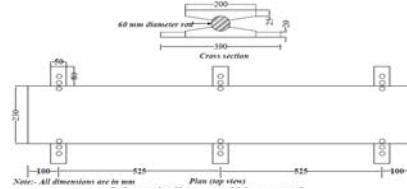

Figure 8(a). Schematic diagram of hinge part

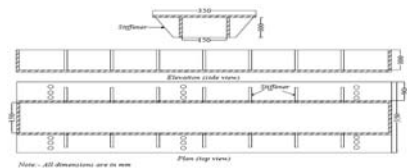Figure 8(b). Schematic diagram of hinge part-1

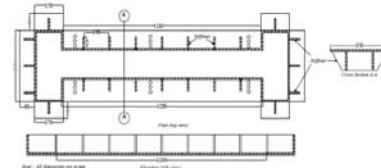Figure 8(c). Schematic diagram of hinge part-2 (plain)

Figure 8(d). Schematic diagram of hinge part-2 (stiffened).

E. Testing Procedure

The panel was placed in the loading frame in the correct position ensuring the end conditions. The wall was then white washed to mark the crack pattern. LVDTs were arranged at their fixed locations. The instruments were checked and adjusted properly, before applying the load. A small load of around 10 kN was first applied to make sure that all the instruments were functioning. The load is then increased gradually with an increment of 50 kN for slender walls and 100 kN for squat walls until the failure. At each load increment, strains in concrete, steel reinforcement and steel connectors were recorded by a Data Logger with catmanEasy supported by HBM connected to a computer. The crack pattern was also noted at each load increment. Cracks were marked on surface of the panel corresponding to the load.

IV. DISCUSSION OF TEST RESULTS

The structural behaviour of the panels was observed by measuring the surface strains of both concrete wythes, steel connectors and steel reinforcement along with lateral deflections at strategic locations on each panel. The performance of each panel is described through axial load bearing capacity, load-deformation response, load - strain curves, influencing of longitudinal reinforcement, influence of stiffeners, cracking pattern and mode of failure.

E. Load deflection response

Fig. 9 depicts the lateral deflection at the mid-height of the panels WP2-NR-AC and WP2-WR-AC under axial loading. At the initial stages of loading, the load-deflection response is nearly linear exhibiting elastic behavior. However, after the crack formation, the panels exhibited non-linear behavior. The maximum deflection was 72.88 mm in panel WP2-NR-AC.
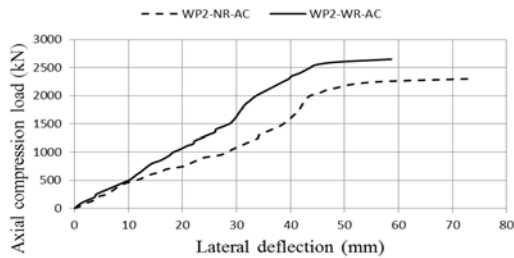

Figure 9. Axial load vs. lateral deflection at mid-height of plain walls.

Compare to plain walls, stiffened walls were deflected less. The lateral deflection at the mid-height of the four panels SWP1-NR-AC, SWP1-WR-AC, SWP2-NR-AC and SWP2-WR-AC under axial loading has been recorded. The load-deflection response is nearly linear at the initial stages of loading. The deflection of panel SWP2 is found to be less significant than that of panel SWP1 as SWP2 has higher slenderness. This is due to the addition of stiffener in the wall panels. The maximum deflection is 4.09 mm for panel SWP2-NR-AC.

Figs. 10(a) and (b) demonstrate the lateral deflections along the height of the walls. The increase in the lateral deflection was noticeable only prior to failure. At the earlier stages of loading, the panels did not deflect much, and the middle part of the wall deflects more. After crack formation, the lateral deflection of the panels at the mid height became higher than that measured at the top and middle of the wall. However, the deflection remained small throughout. In all the panels, both concrete wythes deflected together showing composite behavior.
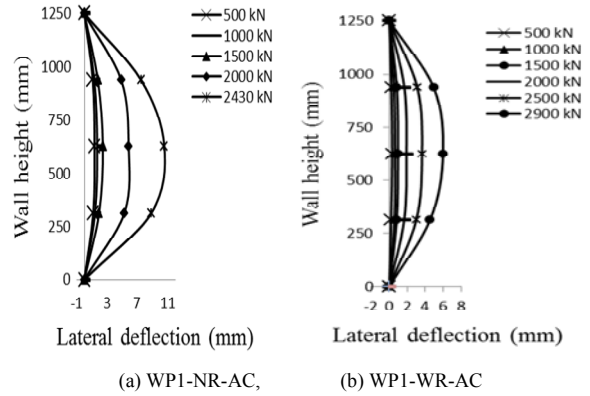

(a) WP1-NR-AC,   (b) WP1-WR-AC

Figure 10. Lateral deflection of wall panels.

The behavior and failure modes of wall panels under axial loading with varying parameters like stiffeners and longitudinal reinforcement bars are also shown in Fig. 11. The displacements were measured by the transducers S_{vf} and S_{vb} positioned in the vertical position on the front and rear faces of the walls. In axially loaded plain wall panels, two concrete layers initially deform same magnitude, which are nothing but shortening deformations. Only during the higher loading phase does the behaviour of two concrete layers become different, with one concrete layer was shortened and the other elongated. In axially loaded stiffened wall panels, the vertical deformation or shortening of the wall was very small.
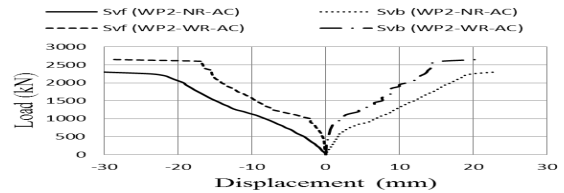

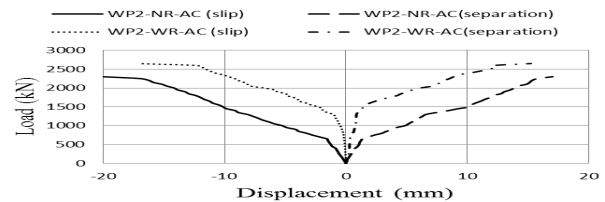Figure 11. Vertical deformation of concrete layers in axial compression (slender wall)

Figure 12. Slip and separation of concrete layers under axial compression (slender wall).

In Fig. 12 the longitudinal displacements between the two concrete layers are plotted with increasing axial loading, are calculated from the vectorial decomposition of the displacement recorded by transducers S_4 and S_5. The longitudinal slip is linear at small load levels, which tends to become non-linear at the ultimate loads. Compared to the slip, the separation is much small in squat walls, revealing that the two concrete layers deflect together, whereas in slender walls the separation is low compared to slip.

F. Strain characteristics

Fig. 13 depicts the surface strain distribution at the mid-height of the 3D panel under axial compression. All panels exhibited almost similar strain variations. At the initial stage of loading, it is observed that there has been only a small discontinuity of the strain on the surface with increasing load. However, the discontinuity has been pronounced at the failure load. This was due to the fact that the cracks did not appear simultaneously on the two wythes of concrete. All the wall panels showed similar response till significant cracking.
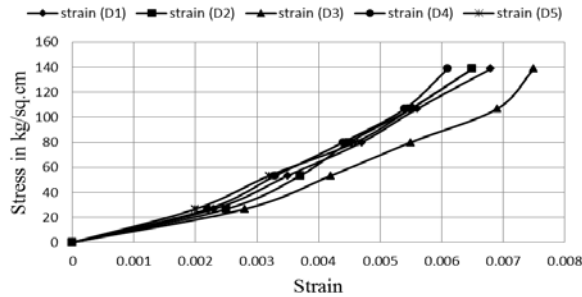

Figure 13. Axial stress vs. surface strain for the specimen WP1-WR-AC

The strains in two adjacent legs of steel connectors vs. axial load near bottom of the panel are presented in Fig. 14. It can be noticed that adjacent legs of the truss connectors developed strains of opposite nature (tension and compression). After the formation of the first crack, the behaviour of the steel connector's legs at the bottom part of the wall, however, could not be clearly explained, as in Fig. 14. This could be due to very small cross sectional area of the connectors. This would result in buckling of the diagonals in compression. Another factor that explains this behaviour could be slippage of steel connectors in the concrete, which can cause flexural stresses near the bend. Similar behaviour was observed when 3D panel was tested under eccentric load [5]. As the strains recorded in the steel reinforcement were all very small and far below the yield strain, only a typical load-strain profile at the mid-height of panel WP2-NR-AC is presented, as shown in Fig. 15.
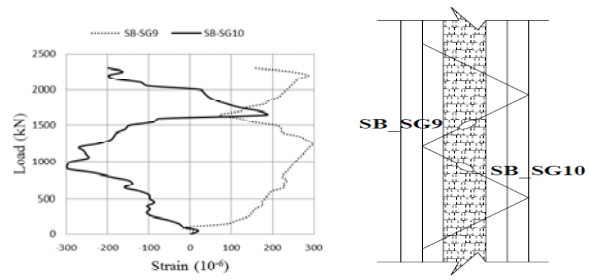

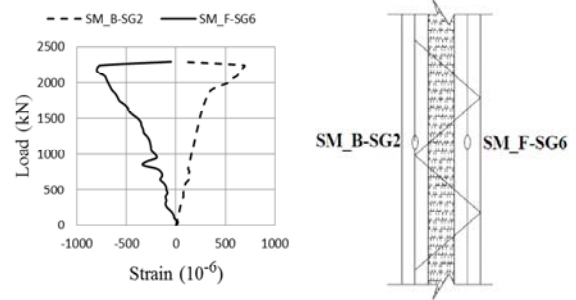Figure 14. Axial load vs. strain in steel (SB-SG9 and SB-SG10) at the bottom of WP2-NR-AC

Figure 15. Axial load vs. strain in steel (SM_B-SG2 and SM_F-SG6) at mid height of WP2-NR-AC

G. Crack patterns and failure mode

The first incremental load of 10 kN was followed by 50 kN increment on slender walls and 100 kN on squat walls. The formation of first cracks and subsequent propagation under further load increments were marked on the wall panels. All the eight panels were tested under axial compression responded in a similar manner. The load corresponding to the appearance of first crack and the failure load were recorded, which are shown in Table V. The first crack was appeared at 1900 kN, 2300 kN, 1800 kN, 2100 kN, 1800 kN, 2000 kN, 1600 kN and 1800 kN respectively in wall panels WP1-NR-AC, WP1-WR-AC, WP2-NR-AC, WP2-WR-AC, SWP1-NR-AC, SWP1-WR-AC, SWP2-NR-AC and SWP2-WR-AC.

TABLE V. CRACK AND FAILURE LOADS OF PANELS UNDER AXIAL LOADING

Wall Panel	Slenderness, H/t	First Crack Load (kN)	% of Ultimate load	Failure Load (kN)[a]	Failure Load (kN/m)[b]
WP1-NR-AC	8.33	1900	78.19%	2430	1944
WP1-WRAC	8.33	2300	79.31%	2900	2320
WP2-NR-AC	25	1800	78.26%	2300	1840
WP2-WR-AC	25	2100	79.24%	2650	2120
SWP1-NR-AC	8.33	1800	51.43%	3500	2800
SWP1-WR-AC	8.33	2000	53.33%	3750	3000
SWP2-NR-AC	25	1600	59.23%	2700	2160
SWP2-WR-AC	25	1800	56.07%	3210	2568

[a] Ultimate strength of panel of 1.25 m width
[b] Ultimate strength of panel of 1 m width

The failure modes that are encountered can be either by material crushing, or by buckling. The plain squat wall WP1-NR-AC was observed to fail by crushing of concrete at the top end, whereas WP1-WR-AC was failed by crushing of concrete at the bottom end (near support), as shown in Fig.16. The plain slender walls WP2-NR-AC and WP2-WR-AC failed due to buckling at the mid height of the wall, also found vertical splitting of panel cross section on sides faces, as shown in Fig. 17. The stiffened squat walls SWP1-NR-AC and SWP1-WR-AC failed due to crushing of concrete both in the wall and in the stiffened portion at the top end (support). The stiffened slender wall SWP2-NR-AC failed due to local crushing of concrete both in the wall and the stiffened portion at the top end, whereas SWP2-WR-AC failed due to local crushing of concrete both in the wall and in the stiffened portion at the bottom (support). Cracks were observed in one or both the concrete wythes and the walls finally failed due to crushing of concrete in squat walls whereas slender walls failed due to buckling. When the load attained the ultimate load, a catastrophic failure was occurred in all cases of crushing and buckling failures at either one end or both the ends.

Figure 16. Figure showing failure of WP1-WR-AC

Figure 17. Figure showing failure of WP2-WR-AC

H. Influence of longitudinal reinforcement

Fig.18 demonstrates the influence of longitudinal reinforcement. The longitudinal reinforcement provided was 0.8% in addition to the wire mesh on both faces of panel along the height. The ultimate strength of panels decreases non-linearity with the increase in the percentage of longitudinal reinforcement. The decrease in strength of panels with P_t = 0.15% to 1.0%, was found to be 16.2% in WP1_AC, 13.2% in WP2_AC, 6.67% in SWP1_AC and 15.88% in SWP2_AC.
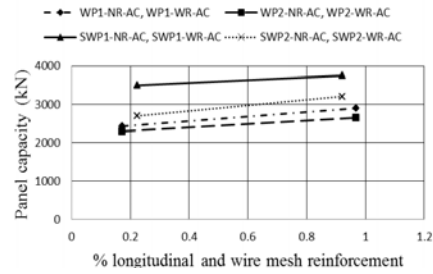

Figure 18. Influence of longitudinal reinforcement.

I. Influence of stiffeners

Fig. 19 shows the ultimate strength of panels with stiffeners. It has been observed that ultimate strength of panels increases with the stiffener both in squat as well as slender walls. The increment of the ultimate strength in SWP1-NR-AC is 30.57% compared to WP1-NR-AC, whereas in SWP1-WR-AC it is 22.67% compared to WP1-WR-AC. In SWP2-NR-AC the ultimate strength is 14.81% compared to WP2-NR-AC, whereas in SWP2-WR-AC it is 17.44% compared to WP2-WR-AC.
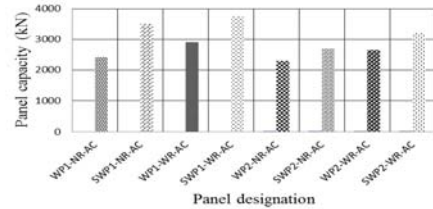

Figure 19. Influence of stiffening elements

V. RESULTS AND FORMULATIONS

The axial load vs. deflection profiles as obtained experimentally at different load stages with varying longitudinal reinforcement and stiffeners. The experimental results are compared with the ACI equation. It can be concluded that the proposed model predicts the deflection with a reasonable accuracy within the elastic stage, whereas the ultimate axial strength of panels was predicted with a good degree of accuracy. The comparison of experimental results with the ACI equation on solid walls and 3D panels are given in Table VI.

Fig 20(a) depicts the comparison of experimental results with ACI equation on squat walls and slender walls. For squat walls with a slenderness ratio of 8.33, the ultimate strength determined by ACI (Eq.(1)) equation is found to be under predicted by around 39%, 48%, 40% and 45% than the experimental ultimate strength of WP1-NR-AC, WP1-WR-AC, SWP1-NR-AC and SWP1-WR-AC respectively. Whereas for slender walls with a slenderness ratio of 25, these differences are increased to 43%, 51%, 42% and 48% as compared to experimental values.

TABLE VI. COMPARISON OF DESIGN STRENGTHS

Panel Designation		Ultimate load (kN)	
	H/t	Eq.(3)	Experiment
WP1-NR-AC	8.33	1470	2430
WP1-WR-AC	8.33	1511	2900
WP2-NR-AC	25	1317	2300
WP2-WR-AC	25	1305	2650
SWP1-NR-AC	8.33	2091	3500
SWP1-WR-AC	8.33	2044	3750
SWP2-NR-AC	25	1560	2700
SWP2-WR-AC	25	1671	3210
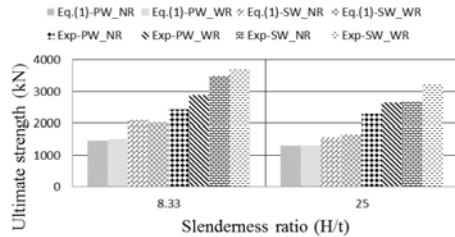
(a) Eq. (1)

Figure 20(a). Comparison of design axial strengths (ACI equation) with experimental result

The slenderness functions $(1 - (kH/32t)^2)$ incorporated in the ACI equation reduces considerably the ultimate capacity for slender wall panels. As a result, the strengths obtained by this equation are conservative when the slenderness ratio is greater than 8.33.

It is worth mentioning that the ACI equation is applicable only if the wall panels behave as composite element, i.e., the steel connectors have sufficient stiffness to promote composite action. The following assumptions and limitations are applicable for the proposed expression:

- The panel acts in a fully composite manner.
- The load on the panel is reasonably concentric, i.e., the resultant must be in the "middle-third" of the overall thickness of the wall. This allows for a maximum eccentricity allowance of t/6.
- The slenderness ratio is limited to 25.

VI. CONCLUSION

The performance of 3D wall panels with slender ness ratio varying between 8.33 and 25.0 under axial compression is reported. The influence of longitudinal reinforcement and stiffeners in 3D wall panels has been observed to be significant on the strength and modes of failure. Cracks were formed in only one layer of concrete or on both. A violent failure occurred in all squat walls due to crushing, whereas in slender walls due to buckling at mid-height. The first cracks were formed at loads in the range of 51-80% of the ultimate loads. The strength of wall panels decreases nonlinearly with increase in the slenderness ratio. The strength reduction was 22.5% in SW_NR when the slenderness ratio was increased from 8.33 to 25.0. Vertical cracks were also observed at the junction of stiffener and wall in SWP1-NR-AC. The strains in steel connectors remained well within the yield limit. The panels behaved as composite members till failure.

REFERENCES

[1] A Brief Introduction into the EVG-3D Panel Constrcuction System (Changing Construction Methods Worldwide)-report on 3D panel.

[2] ACI Committee 318,''Building code requirements for reinforced concrete," (ACI 318-89),Detroit, American Concrete Institute, pp. 111.

[3] A. Benayoune, A.A. Abdul Samad, D.N. Trikha, A.A. Abang Ali, and A.Monayem Akhand, ''Precast reinforced concrete sandwich panel as an industrialised building system," International Conference On Concrete Engg and Technology University Malaya, pp. 1-6, 2004.

[4] A. Benayoune, "Precast concrete sandwich panel as a building system," Ph.D. th, Dept of Civil Engg, Uni. of Putra, Malaysia, 2003.

[5] A. Benayoune, A.A. Abdul Samad, D.N. Trikha, A.A. Abang Ali, and A.A. Ashrabove,''Structural behaviour of eccentrically loaded precast sandwich panels," Construction and Building Materials, Elsevier, vol. 20, pp. 713-724, 2006.

[6] A. Benayoune, A.A. Abdul Samad, D.N. Trikha, and A.A. Abang Ali, ''Behaviour of precast RC sandwich panels with continuous shear truss connectors," Jl. of Inst Eng (Malaysia), v.62(3), pp. 59-66, 2001.

[7] A. Benayoune, A.A. Abdul Samad, A.A. Abang Ali, and D.N. Trikha, ''Response of pre-cast reinforced composite sandwich panels to axial loading," Con and Building Mats, Elsevier, vol. 21, pp. 677-685, 2007.

[8] T.D. Bush and Wu. Zhiqi, "Flexural analysis of PSC sandwich panels with truss connectors," PCI Jl, v. 43(5), pp. 76-86, 1998.

[9] T.D.Bush and G.L. Stine, "Flexural behaviour of composite precast concrete sandwich panels with continuous truss connectors," PCI Journal, vol. 39(2), pp. 112-21, 1994.

[10] A. Einea, D.C.Salmon, M.K. Tadros, and T. Culp, "Partially composite sandwich panel deflection," ASCE, Journal of Structural Engineering, vol. 121(4), pp. 778-83, 1995.

[11] A. Einea, D.C. Salmon, M.K. Tadros, T.Culp, "A new structurally and thermally efficient precast sandwich panel system," PCI Journal, vol. 39(4), p. 90-101, 1994.

[12] A. Einea, "Structural and thermal efficiency of precast concrete sandwich panel system," Ph.D. thesis, Department of Civil Engineering, University of Nebraska-Linkoln, Omaha, NE, 1992.

[13] F. Gara, L. Rangi, D. Roia, and L. Dezi, "Experimental tests and numerical modelling of wall sandwich panels," Engineering Structures, Elsevier, vol. 37, pp. 193–204, 2012.

[14] PCI Com on PC Sandwich Wall Panels, "State of the Art of Precast/prestresses Sandwich Wall Panels," PCI Jl, v. 42(2), pp. 92-133, 1997.